Int J Adv Manuf Technol (2009) 45:496–505
DOI 10.1007/s00170-009-1991-1

ORIGINAL ARTICLE

Effect of process parameters and mathematical model for the prediction of bead geometry in pulsed GMA welding

P. Srinivasa Rao · O. P. Gupta · S. S. N. Murty · A. B. Koteswara Rao

Received: 17 March 2008 / Accepted: 20 February 2009 / Published online: 10 March 2009

Abstract Pulsed gas metal arc welding is one of the most widely used processes in the industry. It offers spray metal transfer at low average currents, high metal deposition rate, versatility, less distortion, and the ability to be used in automated robotic welding systems. The weld bead plays an important role in determining the mechanical properties of the weld. Its geometric parameters, viz., width, reinforcement height, and penetration, are decided according to the welding process parameters, such as wire feed rate, welding speed, pulse current magnitude, frequency (cycle time), etc. Therefore, to produce good weld bead geometry, it is important to set the proper welding process parameters. In the present paper, mathematical models that correlate welding process parameters to weld bead geometry are developed with experimental investigation. Taguchi methods are applied to plan the experiments. Five process parameters, viz., wire feed rate, plate thickness, pulse frequency, pulse current magnitude, and travel speed, are selected to develop the models using multiple regression analysis. The models developed were checked for their adequacy. Results of confirmation experiments show that the models can predict the bead geometry with reasonable accuracy.

P. S. Rao (✉)
Mechanical Engineering,
Vignan's Institute of Engineering for Women,
Visakhapatnam 530046, India
e-mail: psrvizag@yahoo.com

O. P. Gupta · S. S. N. Murty
Mechanical Engineering, Indian Institute of Technology,
Kharagpur, India

A. B. K. Rao
Mechanical Engineering, G V P College of Engineering,
Visakhapatnam, India

Keywords P-GMAW · Bead geometry · Multiple regression · Taguchi method · Analysis of variance (ANOVA)

1 Introduction

The mechanical properties of a weld depend on the chemical composition, thermal history, and bead geometry. For making good welds, it is essential that proper fusion be obtained between the parent metal and the material deposited from the electrode. The surface of the base metal should be thoroughly melted so as to form an arc crater of sufficient depth. If the metal droplets from the electrode and heat of arc are not able to fuse the base metal, shallow crater will result. Figure 1 shows the cross-section of a weld bead and its nomenclature. The weld bead geometry plays an important role in determining the mechanical properties of a weld joint. Its geometric parameters such as bead width, reinforcement height, and depth of penetration depend on the process parameters, such as wire feed rate, welding current, welding speed, plate thickness, etc. Therefore, it is important to set up proper welding parameters to produce a good weld bead. Several studies correlating bead dimensions with process parameters are reported for different welding processes [1]. In most of these studies, the response functions (depth of penetration, bead width, reinforcement height) were expressed as $Y=b_1\ (S)^{b2}\ (I)^{b3}\ (V)^{b4}$ where S is the welding speed, I is the arc current, and V is the welding voltage. And the empirical coefficients, viz., b_1, b_2, b_3, and b_4 are constants which depend on the gas flow rate, wire stick out, and material type. The values of b_1, b_2, b_3, and b_4 were computed by the method of multiple regressions. However, in some studies, the response function was expressed as a linear function of process parameters [2].

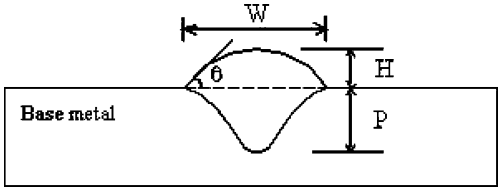

Fig. 1 Weld bead nomenclature. *W* bead width, *H* reinforcement height, *P* depth of penetration, θ wetting angle

Many researchers have developed mathematical models, from the statistically designed experiments, to predict weld bead geometry [2, 3, 5, 7]. Pandey and Parmar [2] have developed models for predicting bead geometry and shape relations for metal inert gas welding of aluminum alloys. The factors considered in these models are wire feed rate, arc voltage, nozzle to work distance, welding speed, torch angle, and flow rate. Senthil Kumar and Parmar [3] developed models for pulsed gas metal arc welding (P-GMAW) to predict weld bead geometry and shape relations as affected by peak current, wire feed rate, pulse duration, welding speed, and plate thickness. Fractional factorial technique was employed to obtain the experimental data. The experimental results were used to develop regression models of the bead geometry. Fractional factorial experiments combined with D-optimal experimental designs were found to be good to improve experimental efficiency [4]. Experimental results showed that the process parameters such as welding speed, arc current, and welding voltage influence the bead characteristics in gas metal arc welding. Kim et al. [5–8] have developed mathematical model for predicting weld width, reinforcement height, and penetration in gas metal arc welding. These models are obtained from regression analysis of experimental data. It is reported that the models can predict the bead geometry within 0–25% accuracy.

Statistical design of experiments (DOE) concept has been successfully applied to many welding situations [9, 10]. However, classical experimental design methods [11, 12] are too complex and a large number of experiments have to be carried out as the number of process parameters increases. In recent years, the Taguchi method [13–15] has become a powerful DOE tool. It provides a simple, efficient, and systematic approach to optimize designs of performance, quality, and cost. Taguchi methods have been adopted [16–18] to analyze the effect of each welding process parameter on the weld pool geometry and to determine the process parameters with optimal weld pool geometry.

2 Experimental equipment

The Fronius Transarc 500 transistorized welding power source is used for depositing beads using pulsed current GMAW. Argon is used as shielding gas. ER70S-6 welding electrode of 1.2-mm diameter is used to deposit bead-on-plate welds on mild steel plates of different thicknesses. The work is fixed on a variable speed tractor and moved beneath the torch. Constant contact tip to workpiece distance (18 mm) is maintained throughout the welding operation. The welding gun is at 90° to the work surface. Test specimens are cut from the weld beads at the middle of the plates. Specimens are ground with abrasive belt grinding machine and polished using standard procedure. Specimens are then etched with 2% NITAL solution. The weld bead characteristics, viz., weld width (*W*), beat height (*H*), and penetration (*P*) are measured with a Tool Maker's microscope.

Table 1 Factors and their levels used in pulsed GMA welding experiments

	Process parameters	Units	Level 1	Level 2	Level 3
A	Plate thickness	mm	6	8	10
B	Frequency	Hz	50	101	152
C	Wire feed rate	m/min	3.0	5.5	8.0
D	WFR/TS ratio	–	15	20	25
E	Peak current	A	440	480	520

Table 2 Experimental layout using L_{18} orthogonal array

Expt. No	Column							
	(1) *e*	(2) Factors	(3)	(4)	(5)	(6)	(7) *e*	(8) *e*
		A	*B*	*C*	*D*	*E*		
1	1	1	1	1	1	1	1	1
2	1	1	2	2	2	2	2	2
3	1	1	3	3	3	3	3	3
4	1	2	1	1	2	2	3	3
5	1	2	2	2	3	3	1	1
6	1	2	3	3	1	1	2	2
7	1	3	1	2	1	3	2	3
8	1	3	2	3	2	1	3	1
9	1	3	3	1	3	2	1	2
10	2	1	1	3	3	2	2	1
11	2	1	2	1	1	3	3	2
12	2	1	3	2	2	1	1	3
13	2	2	1	2	3	1	3	2
14	2	2	2	3	1	2	1	2
15	2	2	3	1	2	3	2	1
16	2	3	1	3	2	3	1	2
17	2	3	2	1	3	1	2	3
18	2	3	3	2	1	2	3	1

Table 3 Experimental results for bead geometry using L_{18} orthogonal array

Bead no.	Bead width (mm)			Reinforcement height (mm)			Depth of penetration (mm)			Convexity index (H/W)
	W_1	W_2	W_{av}	H_1	H_2	H_{av}	P_1	P_2	P_{av}	
E 01	5.02	5.78	5.4	3.0	2.91	2.95	1.55	1.33	1.44	0.546
E 02	11.12	11.76	11.44	2.84	2.82	2.83	3.04	2.79	2.91	0.247
E 03	16.37	15.75	16.06	3.16	2.97	3.06	4.79	5.38	5.08	0.190
E 04	7.47	6.22	6.84	3.82	3.71	3.76	1.75	1.67	1.71	0.549
E 05	15.0	15.12	15.06	2.75	3.63	3.19	2.46	2.02	2.24	0.212
E 06	9.52	9.55	9.53	2.97	2.43	2.7	3.07	3.13	3.1	0.283
E 07	5.37	5.88	5.62	3.85	3.66	3.75	2.73	2.76	2.74	0.667
E 08	11.89	11.83	11.86	3.05	2.92	2.98	3.29	3.71	3.5	0.251
E 09	7.79	9.09	8.44	3.27	3.96	3.61	1.58	1.65	1.61	0.428
E 10	16.29	16.58	16.43	3.32	3.57	3.44	5.19	5.3	5.24	0.209
E 11	7.0	6.59	6.79	3.05	3.66	3.35	1.31	1.19	1.25	0.493
E 12	12.34	13.11	12.72	2.22	2.73	2.47	2.15	2.41	2.28	0.194
E 13	11.31	13.19	12.25	4.11	4.08	4.09	2.96	2.99	2.97	0.334
E 14	6.95	9.95	8.45	3.11	2.56	2.83	3.15	3.20	3.17	0.335
E 15	5.15	5.71	5.43	4.38	4.76	4.57	1.3	1.43	1.36	0.842
E 16	9.78	9.98	9.88	3.68	2.67	3.17	3.84	3.84	3.84	0.321
E 17	8.68	9.5	9.09	4.13	4.34	4.23	1.79	1.38	1.58	0.465
E 18	8.56	9.14	8.85	2.91	2.72	2.81	2.23	2.43	2.33	0.317

3 Design of experiments

The process parameters selected for the present study are plate thickness, pulse frequency (or cycle time), wire feed rate, ratio of wire feed rate to travel speed, and peak current. The ratio of wire feed rate to travel speed (WFR/TS) is chosen as a factor instead of travel speed to avoid the erratic combinations such as high travel speed for low feed rate. Three levels are chosen for all the process parameters (also called factors). The levels for different parameters were established on the basis of preliminary studies conducted. These selected factors and their levels are given in Table 1.

There are 2 degrees of freedom (DOF) for each factor and thus total 10 degrees of freedom for the five process parameters. No interaction is considered between the factors. Therefore, the DOF of the orthogonal array should be greater than 10. In the present study, a L_{18} ($2^1 \times 3^7$) orthogonal array is used. From the linear graph, it was observed that no specific interaction columns are available in a L_{18} orthogonal array. The layout of the L_{18} orthogonal array and factor assignment to columns is given in Table 2. Factor A is assigned to column 2, as this is independent of machine variables. Other factors, B, C, D, and E, are assigned in the order of difficulty in setting them on the welding machine.

4 Experimental procedure

It can be observed from Table 2 that there are a number of combinations of frequency (f), WFR, and peak current (I_p). It

Table 4 Results of ANOVA for depth of penetration

Factors	DOF	Sum of squares	Mean square	Variance ratio F	Percentage contribution	Prob (F)
A (plate thickness)	2	1.1769	0.5885	5.3948	4	0.0382
B (pulse frequency)	2	0.9338	0.4669	4.2803	2.98	0.0611
C (wire feed rate)	2	18.8046	9.4023	86.1949	77.49	0.0000
D (WFR/TS ratio)	2	1.8997	0.9499	8.7079	7.01	0.0126
E (peak current)	2	0.4062	0.2031	1.8618	0.78	0.2247
(error)	7	0.7636	0.1091		7.73	
Total	17	23.9848	1.4109			

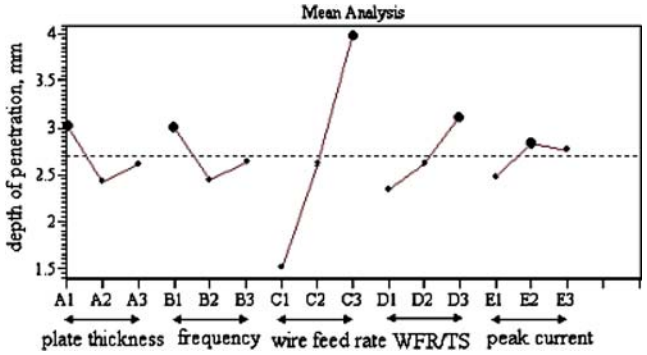

Fig. 2 Effect of factor levels on depth of penetration

is required to obtain the stable pulse parameter settings for each of the 18 combinations. For a given combination of frequency, wire feed rate and peak current (i.e., cycle time, average current, and peak current), the peak duration (T_p), and background current are adjusted to obtain the stable spray mode of metal transfer. For example, at 50-Hz frequency (cycle time—20 ms) and wire feed rate of 3.0 m/min, all the three levels of peak current, i.e., 440, 480, 520 A, are to be selected. This is achieved by varying the peak duration (T_p) to match with burnoff rate. At high wire feed rates, varying T_p alone is not sufficient to obtain the required burnoff rate. So in such cases, background current is increased to obtain stable metal transfer by matching the burnoff rate with wire feed rate.

The current and voltage waveforms are recorded for all the experiments. These waveforms are used in selecting the proper combinations of pulse parameters for spray mode of metal transfer. A number of trials are performed in order to ensure that the selected parameter combination would result in spray metal transfer. The experiments are conducted in random order to protect from any unknown and uncontrolled factors that may vary during experiments.

The plates are cut, leaving 1 in. from trailing edge of the plate to avoid end effects. Two specimens at different sections are taken from each bead and the surfaces are ground and polished using standard metallography procedure. The surfaces are then etched with 2% NITAL. The bead dimensions, viz., bead width, reinforcement height, depth of penetration, are measured with a Tool Maker's microscope. The convexity of the bead is estimated by the following ratio:

Convexity index=Reinforcement height (H)/Weld width (W).

5 Results of orthogonal array experiments

The bead width (W), reinforcement height (H), and depth of penetration (P) of all the beads are measured. The average values of each bead W_{av}, H_{av}, and P_{av} are computed. Convexity index of the beads is computed using W_{av} and H_{av}. The results for all the beads are given in Table 3.

The optimum level for a factor is the level that gives the desired quality characteristics in the experimental region. The desired quality characteristic for penetration is *the-bigger-the-better*, and for convexity index, the desired quality characteristic is *the-smaller-the-better*. The relative contributions of the factors are determined from the analysis of variance (ANOVA) table.

5.1 Analysis of variance

The purpose of analysis of variance is to investigate process parameters that significantly affect the desired performance characteristic. This is accomplished by separating the total variability of the response into contributions by each of the process parameters and the error. The total sum of squared deviation SS_T is decomposed into two sources: the sum of the squared deviations SS_d due to each process parameter and the sum of squared error SS_e. The percentage contribution by each of the process parameters in the total sum of the squared deviations SS_T can be used to evaluate the importance of the process parameter change on the performance characteristic.

The variance ratio, denoted by F, is the ratio of the mean square due to a factor and the error mean square. A large value of F means that the effect of that factor is large compared to the error variance. Also, the larger the value of F, the more significantly that factor is influencing the performance characteristic (i.e., penetration, convexity).

5.1.1 ANOVA for depth of penetration

An ANOVA analysis for estimating the error variance for the factors is given in Table 4. The values of sum of the squares due to various factors, tabulated in the third column of Table 4, are a measure of relative importance of the factors in changing the depth of penetration. It is observed that the wire feed rate contributes a major portion (77.49%) of the total variation. WFR/TS ratio has the next highest contribution (7.01%). Base plate thickness and frequency together are contributing only a small portion, i.e., 4% and

Table 5 Mean analysis for depth of penetration

	A	*B*	*C*	*D*	*E*
Level 1	3.0333	2.99	1.4917	2.3383	2.4783
Level 2	2.425	2.4417	2.5783	2.6	2.8283
Level 3	2.6	2.6267	3.9883	3.12	2.7517
Delta	0.6083	0.5483	2.4967	0.7817	0.35
Rank	3	4	1	2	5
SD 1.1878					

Table 6 Results of ANOVA for convexity index

Factors	DOF	Sum of squares	Mean square	Variance ratio *F*	Percentage contribution	Prob (*F*)
A (plate thickness)	2	0.0441	0.022	1.5271	2.73	0.2816
B (pulse frequency)	2	0.0328	0.0164	1.1351	0.7	0.3741
C (wire feed rate)	2	0.2767	0.1383	9.5902	44.45	0.0099
D (WFR/TS ratio)	2	0.0567	0.0284	1.9666	5	0.2100
E (peak current)	2	0.0464	0.0232	1.6075	3.14	0.2664
(error)	7	0.101	0.0144		43.98	
Total	17	0.5576	0.0328			

2.98%, respectively. Peak current has little contribution (0.78%) in the total variation of penetration.

In addition, the *F* test is also used to determine process parameters that have significant effect on performance characteristic. Usually, an *F* value larger than four indicates that the factor effect is quite large [13]. It is observed that the *F* values of factors A, B, C, and D are more than 4. Thus, the four factors, WFR, WFR/TS ratio, plate thickness, and frequency, have a significant effect on the depth of penetration.

5.1.2 Analysis of results for depth of penetration

From the experimental results of the 18 experiments in Table 3, it is observed that the mean penetration ranges from 1.25 to 5.24 mm. Also, the variation in convexity index ranges from 0.190 to 0.842. A summary of factor effects is tabulated in Table 4. The penetration value 3.0333 is the average of penetrations obtained in the selectively chosen experiments out of the 18 experiments for plate thickness values of 6 mm, which is at level 1 for factor A. The other mean penetrations are also obtained in the same way. Delta is the variation of the mean values of penetration within that factor. The effect of factors is ranked as per the magnitude of delta values. The highest ranked factor "C" has the maximum effect, followed by D, A, B, and E in order. The factor effects are displayed graphically in Fig. 2, which makes it easy to visualize the relative effects of the various factors on depth of penetration.

Table 7 Mean analysis for convexity index

	A	*B*	*C*	*D*	*E*
Level 1	0.3132	0.4377	0.5538	0.4402	0.3455
Level 2	0.4258	0.3338	0.3285	0.4007	0.3475
Level 3	0.4082	0.3757	0.2648	0.3063	0.4542
Rank	3	5	1	2	4
SD 0.1811					

The following observations are made from Fig. 2 and Table 5:

(a) Wire feed rate (factor C) has the largest effect on depth of penetration. By increasing the feed rate from 3 to 8 m/min, the depth of penetration can increases by 2.49 mm.
(b) The wire feed rate to travel speed ratio (factor D) has the next largest effect on depth of penetration. Increasing the WFR/TS ratio from 15 to 25, i.e., reducing the travel speed, can improve depth penetration by 0.78 mm.
(c) Plate thickness (factor A) has mixed effect on the depth of penetration. The mean depth of penetration is low on 8-mm plate. Depth of penetration is more on 6-mm-thick plate. The change in penetration depth is about 0.6 mm.
(d) Pulse frequency (factor B) has mixed effect as that of factor A on depth of penetration. The mean penetration is high at frequency level 1 and low at frequency level 2. The range of change in penetration depth is about 0.55 mm.
(e) Peak current (factor E) has little effect on the depth of penetration among the factors considered in the present study.

In the present analysis, since the depth of penetration is the response variable, the higher value of quality charac-

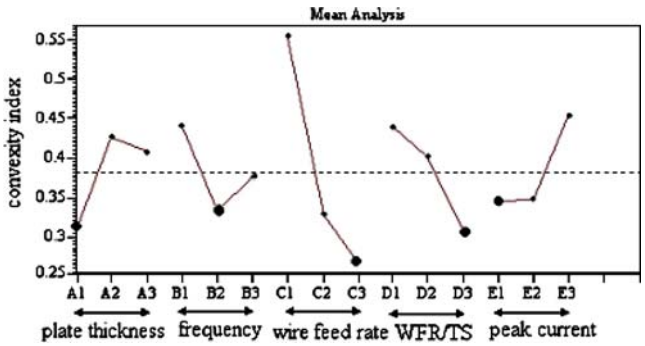

Fig. 3 Effect of factor levels on convexity index

Table 8 Results of confirmation experiments (with $A_1B_2C_3D_3E_1$)

Bead	Width (mm)		Height (mm)		Average value		Convexity index	
No.	W_1	W_2	H_1	H_2	W_{av}	H_{av}		
E19a	15.23	14.89	3.08	3.2	15.06	3.14	0.208	Average 0.199; SD 0.0103
E19b	16.75	16.05	3.21	2.96	16.4	3.085	0.188	
E19c	15.89	15.97	3.34	3.1	15.93	3.22	0.202	

teristic is better. Therefore, from Fig. 2, the optimum conditions chosen are $A_1B_1C_3D_3E_2$.

5.1.3 ANOVA for convexity index

An ANOVA analysis for estimating the error variance for the factors is given in Table 6. The sum of the squares values due to various factors, tabulated in the third column of Table 6, are a measure of the relative importance of the factors in changing the convexity index (C.I). It is observed that the wire feed rate contributes a major portion (44.45%) of the total variation. WFR/TS ratio has the next highest contribution (5%). Peak current and plate thickness together are contributing only a small portion, i.e., 3.14% and 2.73%, respectively. Pulse frequency has little contribution (0.78%) in the total variation of convexity index.

The F value of factor C is higher among all the factors; this factor C (wire feed rate) has the most significant effect on convexity index of a bead. The F values of all other factors are more than one but less than two. An F value of more than 1 means that the factor effect is greater than experimental error [13].

5.1.4 Analysis of results for convexity index

It is observed from the results tabulated in Table 3 that the mean convexity index ranges from 0.190 to 0.842. A summary of factor effects is tabulated in Table 7 and the factor effects are displayed graphically in Fig. 3, which makes it easy to visualize the relative effects of the various factors on convexity index.

The following observations are made from Fig. 3 and Table 7:

(a) Wire feed rate (factor C) has the largest effect on convexity index. By increasing the feed rate (average current) from 3 to 8 m/min, the convexity index has reduced by about 0.289.
(b) The wire feed rate to travel speed ratio (factor D) has the next largest effect on convexity index. Increasing the WFR/TS ratio from 15 to 25, i.e., reducing the travel speed, can reduce the convexity index by 0.134.
(c) Plate thickness (factor A) has mixed effect on the convexity index. The mean convexity index is high on 8-mm plate. Convexity is low on 6-mm-thick plate. The change in convexity index is 0.1127
(d) With increase in peak current (factor E) magnitude, the C.I increases. C.I is particularly high at high peak current magnitude. The variation in the convexity index is about 0.1087
(e) Pulse frequency (factor B) has mixed effect on the convexity index. Mean value of C.I is minimum at 100-Hz frequency and maximum at low frequency (50 Hz). Mean C.I is also more at high frequency (150 Hz).

As the lower value of convexity index is better, it is observed from the graph (Fig. 3) that the optimum conditions for lower C.I are $A_1B_2C_3D_3E_1$.

6 Confirmation experiments

Conducting a confirmation experiment is a crucial step in the DOE process. A set of confirmation experiments is performed by using a specific combination of the factor levels obtained from the analysis described in the previous section. Its purpose is to verify that the optimum conditions suggested by the matrix experiment do indeed give the projected improvement. If the observed values under the optimum conditions are close to their respective predictions, then we conclude that the additive model on which the matrix experiment is based is a good approximation of

Table 9 Analysis of variance for depth of penetration model

Source	DOF	Sum of squares	Mean square	Variance ratio F	Prob (F)
Regression	5	0.4222	0.0844	7.48	0.0021
Error	12	0.1353	0.0112		
Total	17	0.5576			

Table 10 Analysis of variance for convexity index model

Source	DOF	Sum of square	Mean square	Variance ratio F	Prob (F)
Regression	5	22.6155	4.5231	39.64	0.000
Error	12	1.3692	0.1141		
Total	17	23.9848			

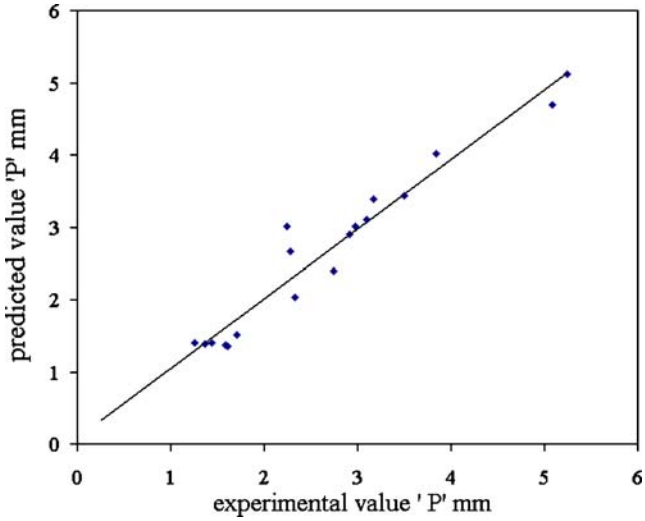

Fig. 4 Predicted values vs experimental values of depth of penetration

the reality. Then, we adopt recommended optimum conditions for our process.

It is observed from the Fig. 2 that the optimum combination of parameters for higher penetration (the-higher-the-better) is $A_1B_1C_3D_3E_2$. Therefore, the confirmation experiments are to be conducted with the parameters: base plate thickness—6 mm, frequency—50 Hz, wire feed rate—8.0 m/min, WFR/TS ratio—25, and peak current—480 A. It can be seen from the experimenters log sheet that this parameter combination is the same as the experiment run no. E10. It is observed from the experimental results in Table 3 that the average depth of penetration for E10 is 5.24 mm, which is highest among all the experiments.

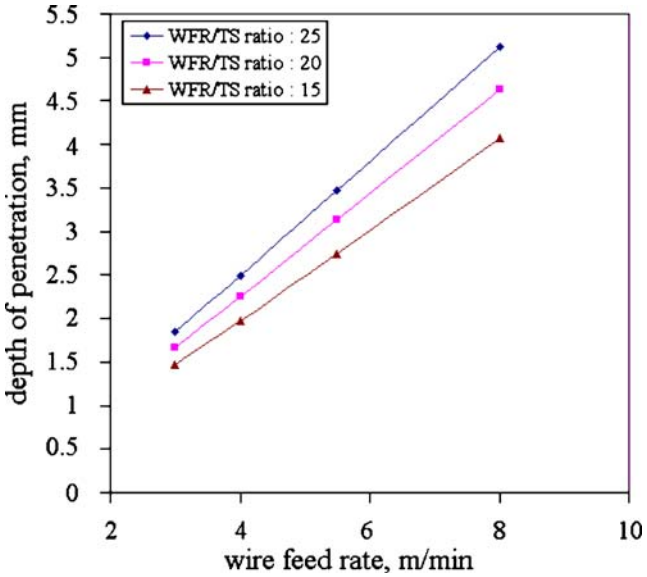

Fig. 5 Predicted depth of penetration at different wire feed rates (on 6-mm-thick plate)

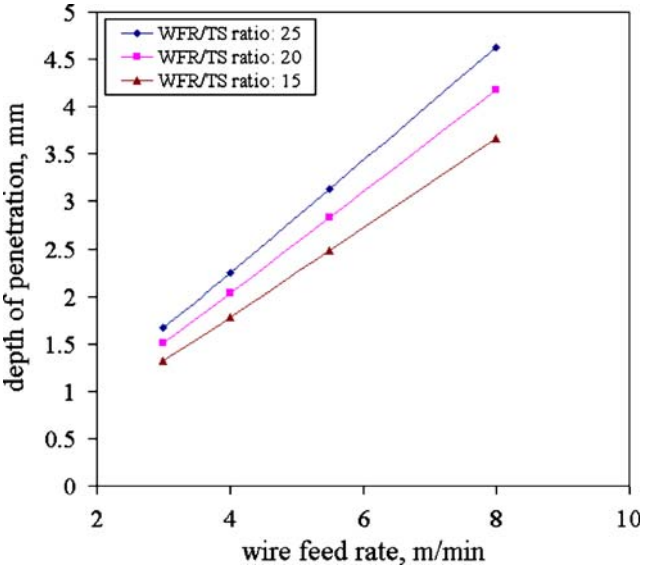

Fig. 6 Predicted depth of penetration at different wire feed rates (on 8-mm-thick plate)

Hence, no separate confirmation tests are required for this set of optimum combination.

It is observed from Fig. 3 that the optimum combination of parameters for low convexity index (lower the better) is $A_1B_2C_3D_3E_1$. This combination of parameters does not exist in the experimenter log sheet. Therefore, confirmation experiments are required to be conducted with this combination, i.e., plate thickness—6 mm, frequency—100 Hz, wire feed rate—8.0 m/min, WFR/TS ratio—25, and peak current—480 A. The experimental results obtained are shown in Table 8. It is confirmed from Table 8 that the average convexity index is lower with the factor

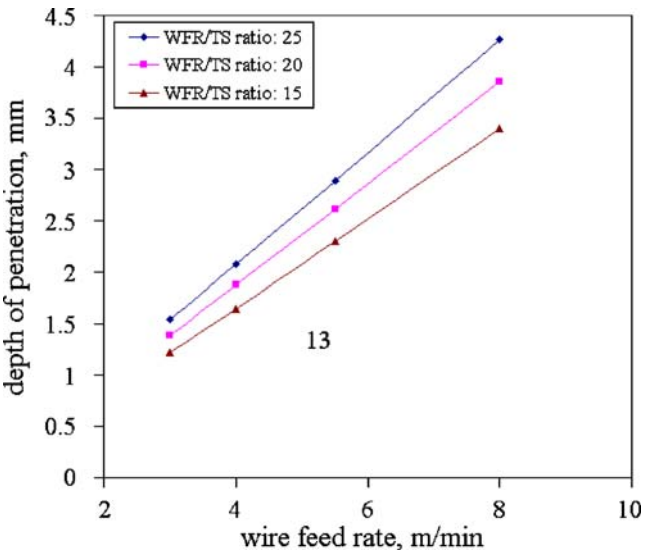

Fig. 7 Predicted depth of penetration at different wire feed rates (on 10-mm-thick plate)

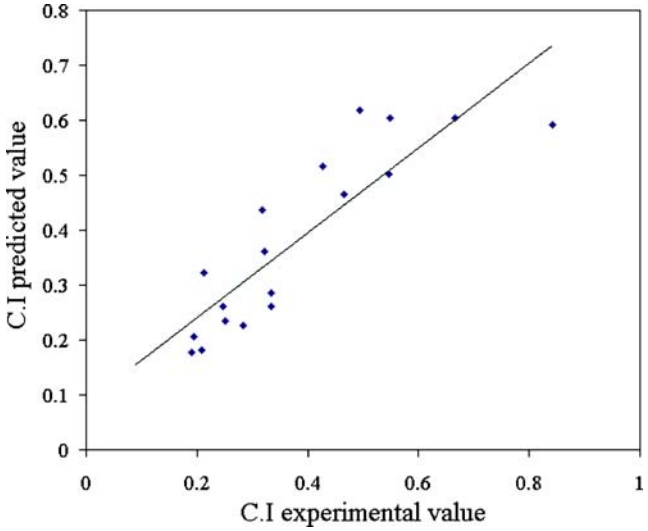

Fig. 8 Predicted values vs experimental values of convexity index

levels at $A_1B_2C_3D_3E_1$. This is comparable with the results in Table 3, as factors B and E have the least effect.

7 Development of mathematical models

The experimental results that are given in the previous section are used to obtain the mathematical relationship between process parameters and bead geometry. The coefficients of mathematical models are computed using method of multiple regressions. Datafit software [19] has been used for the regression analysis. This software is used to test several models, viz., linear, exponential, power series (user-defined). Out of all models tested, the model that has high coefficient of multiple determination (R^2) value and better t ratio is chosen. The adequacy of the models and the significance of coefficients are tested by applying analysis of variance and Student's t test.

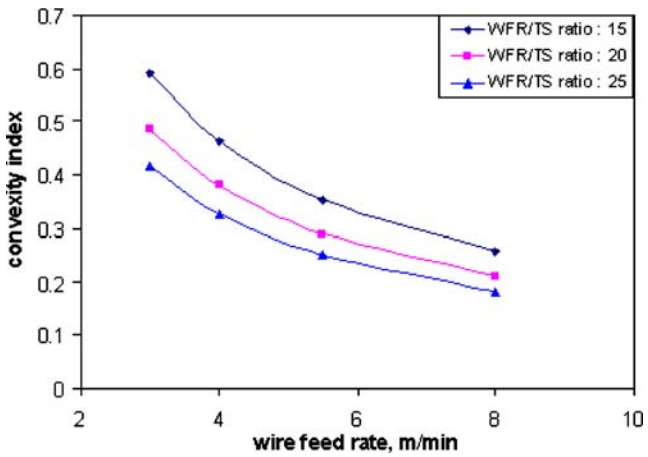

Fig. 9 Predicted convexity index at different wire feed rates (on 6-mm-thick plate)

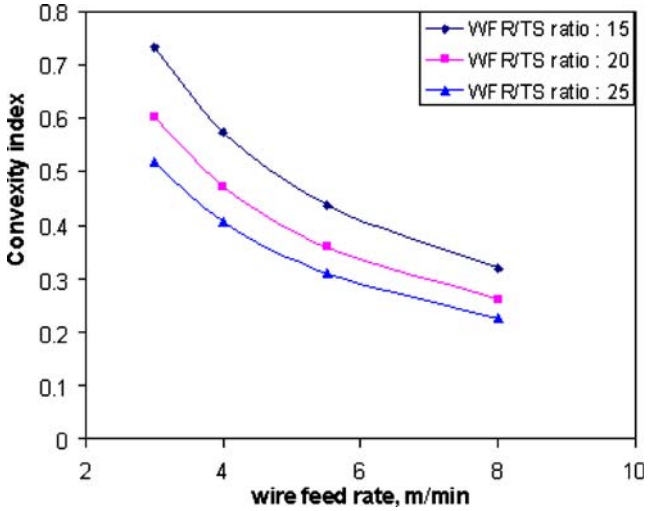

Fig. 10 Predicted convexity index at different wire feed rates (on 8-mm-thick plate)

The relationship between response variable(s) (penetration or convexity index) and process parameters (viz., plate thickness, pulse frequency, wire feed rate, WFR/TS ratio, peak current) can be expressed as:

$$Y = 10^a X_1^b X_2^c X_3^d X_4^e X_5^f$$

where Y is the penetration in millimeters or convexity index

X_1 — plate thickness (mm, factor A)
X_2 — pulse frequency (Hz, factor B)
X_3 — wire feed rate (m/min, factor C)
X_4 — wire feed rate/travel speed ratio (factor D)
X_5 — peak current (A, factor E)
a, b, c, d, e, and f — regression variables.

Multiple regression analysis is performed using the experimental data given in Table 3. Different models are

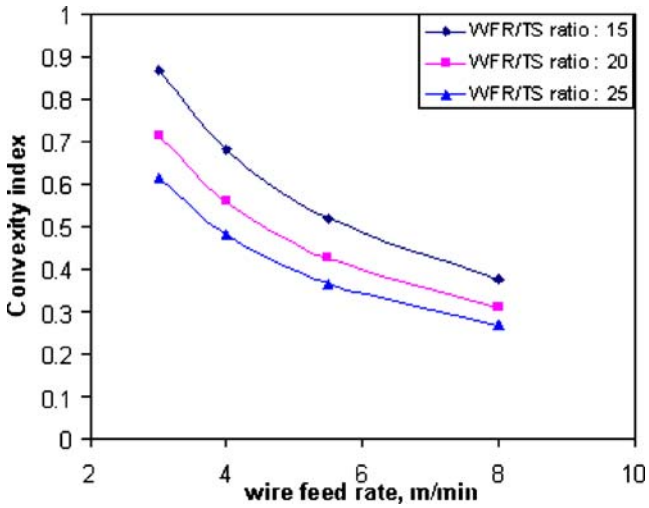

Fig. 11 Predicted convexity index at different wire feed rates (on 10-mm-thick plate)

tested and the model that has high coefficient of multiple determination (R^2) value is selected. The regression variables a, b, c, d, e, and f are obtained as follows:

$$\text{Depth of penetration } P = \frac{X_3^{1.0401} X_4^{0.4516} X_5^{0.4731}}{10^{1.6625} X_1^{0.3545} X_2^{0.1126}} \quad (1)$$

$$\text{Convexity index } C.I = \frac{X_1^{0.7498} X_5^{1.9137}}{10^{4.4695} X_2^{0.1554} X_4^{0.6826}}. \quad (2)$$

Results of regression analysis for depth of penetration and C.I are analyzed. The adequacy of the each model is tested by the ANOVA. Tables 9 and 10 show the ANOVA for P and C.I models, respectively.

Figure 4 shows the relationship between experimental values and those predicted for depth of penetration in conventional pulsed gas metal arc welding. It is observed from the figure that the values predicted by penetration model are in good agreement with experimental values. It is observed that the percentage error is less than 16% in all the cases except with one. Hence, it is concluded that the model can be used to predict the depth of penetration in conventional P-GMAW with good accuracy.

The predicted depth of penetration in P-GMAW at different wire feed rates are plotted in Figs. 5, 6, and 7 for 6-, 8-, and 10-mm-thick plate, respectively. The optimum parameter combination for maximum penetration was obtained as $A_1B_1C_3D_3E_2$. So the values of pulse frequency and peak current are taken as 50 Hz and 480 A, respectively, for plotting predicted depth of penetration at different wire feed rates, WFR/TS ratio, and on different plate thicknesses. It is observed from the plots that the depth of penetration increases with an increase in wire feed rate or a decrease in welding speed (i.e., increase in WFR/TS ratio) for a given plate thickness. This is because at high wire feed rate, the heat input is more and hence more depth of penetration. Similarly, at high WFR/TS ratio (low welding speed), the rate of heat input on to the weld pool is more, which results in more depth of penetration for a given plate thickness. Figures 5, 6, and 7 are useful in predicting the depth of penetration at different wire feed rates and at different WFR/TS ratios.

Figure 8 shows the relation between experimental values and those predicted for convexity index in conventinal pulsed gas metal arc welding. It is obsereved from the figure that the values predicted by the model are in reasonbly good agreement with experimental values. The predicted and experimental values and percentage error are compared, and it is observed that the percentage error is less than 15% in most of the cases except a few. Figures 9, 10, and 11 can be used to predict the convexity index at different wire feed rates and at different WFR/TS ratios.

8 Conclusions

- The bead geometry is mainly influenced by wire feed rate and WFR/TS ratio in pulsed gas metal arc welding.
- High mean current, i.e., high wire feed rate with low travel speed, will result in high penetration and low convexity of the bead.
- Finger type pentration is predominant in P-GMAW. At low mean currents, the convexity is high in pulsed gas metal arc welding.
- The depth of penetration is better at low pulse frequency, i.e., 50 Hz compared to other pulse frequency levels.
- Convexity is high at low and high pulse frequencies and is miminum at 100 Hz.
- High peak current results in high convexity. This is because at high peak current, the peak duration is less (for the same mean current), which will result in quick cooling of weld pool.
- Penetration is more at high peak current because of high arc force.
- Confirmation tests revealed that beads with low convexity can be obtatined by selecting appropriate parameters ($A_1B_2C_3D_3E_1$).
- The optimum bead geometry can be obtained by selecting high wire feed rate, low travel speed on thin base plate. The pulse frequency and peak current are to be selected suitably depending on thickness of base plate.
- The mathematical models developed can predict the depth of penetration and convexity index in conventional P-GMAW with good accuracy.

References

1. McGlone JC (1982) Weld bead geometry prediction—a review. Met Constr 14:378–384
2. Pandey S, Parmer RS (1989) Mathematical models for predicting bead geometry and shape relationships for MIG welding of aluminum alloy 5083. Proceedings of the 2nd International Conference on Trends in Welding Technology USA, 14–18 May, pp 37–41
3. Senthil Kumar R.and Parmar RS (1986) Weld bead geometry prediction for pulse MIG welding. Proceedings of an International Conference on Trends in Welding Technology, USA, 18–22 May, pp 647–652
4. Subramaniam S, White DR, Lones JE, Lyons DW (1999) Experimental approach to selection of pulsing parameters in pulsed GMAW. Weld J 78(5):166–172
5. Kim IS, Kwon WH, Siores E (1996) An investigation of a mathematical model for predicting weld bead geometry. Can Metall Q 35(4):385–392. doi:10.1016/S0008-4433(96)00012-2
6. Kim IS, Park CE, Jeong YJ, Son JS (2001) Development of an intelligent system for selection of the process variables in gas

metal arc welding processes. Int J Adv Manuf Technol 18:98–102. doi:10.1007/s001700170080
7. Kim IS, Son JS, Kim IG, Kim JY, Kim OS (2003) A study on relationship between process variables and bead penetration for robotic CO_2 arc welding. J Mater Process Technol 136:139–145. doi:10.1016/S0924-0136(02)01126-3
8. Kim IS, Son KJ, Yang YS, Yarlagada PKDV (2003) Sensitive analysis for process parameters in GMA welding processes using a factorial design method. Int J Mach Tools Manuf 43:763–769. doi:10.1016/S0890-6955(03)00054-3
9. Ramaswamy S, Gould J, Workman D (2002) Design-of-experiments study to examine the effect of polarity on stud welding. Weld J 81(2):19–26s
10. Allen TT, Richardson RW, Tagliabue DP, Maul GP (2002) Statistical process design for robotic GMA welding of sheet metal. Weld J 81(5):69–77s
11. Montogomory DC (2001) Design and analysis of experiments, 5th edn. Wiley, New York
12. Weber DC, Skillings JH (2000) A first course in the deign of experiments. CRC, Boca Raton
13. Phadke MS (1989) Quality engineering using robust design. Prentice Hall, Englewood Cliffs, New Jersey
14. Ross PJ (1996) Taguchi techniques for quality engineering, 2nd edn. McGraw-Hill, New York
15. Bendell T (ed) (1988) Taguchi methods. Proceedings of the 1988 European Conference, Elsevier Applied Science, London
16. Jaung SC, Tarng YS (2002) Process parameter selection for optimizing the weld pool geometry in the tungsten inert gas welding of stainless steel. J Mater Process Technol 122:33–37. doi:10.1016/S0924-0136(02)00021-3
17. Tarng YS, Yang WH, Juang SC (2000) The use of fuzzy logic in the Taguchi method for the optimization of the submerged arc welding process. Int J Adv Manuf Technol 16:688–694. doi:10.1007/s001700070040
18. Xue Y, Kim IS, Park CE (2004) Application of Taguchi's method on the optimized bead geometry in the gas metal arc welding. Proceedings of the 3rd International Conference on Advanced Manufacturing Technology (ICAMT 2004), Kuala Lumpur, 11–13 May, pp 771– 776
19. DATAFIT 8.0.32 (2004) User manual. Oakdale Engineering, USA